Joint Time-Frequency Analysis of Ultra Wideband Radar Signals

Hoi-Shun Lui, Nicholas V. Z. Shuley

School of Information Technology and Electrical Engineering
The University of Queensland, Brisbane 4072, Australia
Email: lui@itee.uq.edu.au

***Abstract*- The time variant nature of an Ultra-Wideband (UWB) radar signal scattered from a radar target is well described throughout the literature. To study the behaviour of these transient signals, Joint Time-Frequency (TF) analysis is considered. Various Time-Frequency Distributions (TFDs) have been developed in the signal processing area over the last twenty years but little work has been done in a UWB context. In particular, the main objective of this paper is to study the transient electromagnetic scattering phenomena from a metallic radar target in free space. Numerical examples using a bent wire target will be presented to demonstrate the feasibility of using TFDs to study the electromagnetic scattering phenomena embedded in the target response.**

I. INTRODUCTION

Standard Fourier analysis decomposes a time domain signal into individual frequency components. The Fourier Transform assumes that all the frequency components occur at the same time, but this does not provide any information about their occurrence. As a result, Fourier analysis is only suitable for analyzing stationary signals. For signals with time-varying frequency content, one way to study their behaviour is with Time-Frequency (TF) signal analysis [1-4]. In TF analysis, the signals (either in time or frequency domain) are transformed to the Joint Time-Frequency domain, and they are represented in two dimensional TF space. The development of the frequency components can be easily observed visually. One of the first applications using TF analysis applied a moving window to the signal in the time domain and then Fourier transformed the result to the frequency domain. The resultant distribution is known as the Short-Time Fourier Transform (STFT). The magnitude of the STFT is known as the Spectrogram (SP), which was first applied to analyzing audio signals in the 1940s [1].

One of the well-known shortcomings of the STFT is that it is not able to achieve fine time and frequency resolution simultaneously due to the constraint of the uncertainty principle [1-2]. In other words, if one would like to achieve fine resolution in the time domain, the resolution in the frequency domain would be correspondingly degraded and vice versa. One way to handle this resolution issue is to use the Wigner-Ville Distribution (WVD) [1-4]. The WVD is capable of producing the best time-frequency resolution compromise of all the Time-Frequency Distributions (TFDs); however, the price paid is termed "cross-term interference" [5]. Such cross terms usually do not provide any physical interpretation of the signal and extensive work has been carried out to suppressing these cross terms. For example, one method smoothes the WVD using particular time and frequency windows thus resulting in the Pseudo Wigner-Ville Distribution (PWVD) or the Smooth Pseudo Wigner-Ville Distribution (SPWVD) [5]. The variants of the WVD utilize special kernels that reduce the cross terms [6-9].

Joint TF analysis has been widely applied to various engineering applications such as signal processing in biomedical applications, speech processing, wireless communication, radar and sonar applications. In radar applications, in particular for stationary targets, most work has been carried out on narrow-band applications [10]. For UWB radar, there has been some work on feature extraction [11-12] and quite a substantial amount of work done by H. Ling [13-15] on TF analysis of backscattered signals as well as range profiles for stationary targets. The frequency range of operation is in the quasi-optical region which lies beyond the fundamental resonant modes and interest is focused rather on high frequency scattering phenomena such as diffraction from edges and corners. Such phenomena can be described by the Geometric Theory of Diffraction (GTD) in the electromagnetic context [16].

In this paper, instead of high frequency behaviour, the focus is on studying the scattering phenomena of a radar target in the resonant region using various TFDs. The excitation frequency is on the scale of about 3 to 10 wavelength of the fundamental resonant mode of the target. For Perfectly Electric Conductor (PEC) targets with a size of few centimetres up to a few metres, this corresponds to frequencies in the range of few hundred MHz up to a few GHz, and is classed as UWB. With such an excitation frequency band, the dominant scattering phenomena are resonances that correspond to the physical structure as well as the dielectric properties of the target. These target resonances appear in the late time of the target response. It is well known from the literature that these late time target resonances are theoretically target dependent and aspect independent [17-18]. Extensive work has been carried out towards using these complex resonances as a feature set for target recognition, for example, the E-Pulse and S-Pulse technique [18-19].

This paper outline is as follows: In the next section some background on transient electromagnetic scattering is given, followed by a review of TFDs. In section IV, a numerical example of a bent wire target is presented to demonstrate the feasibility of using TFDs to study transient electromagnetic scattering and conclusions are reached at the end of the paper.

II. UWB TRANSIENT ELECTROMAGNETIC SCATTERING

Studies on transient electromagnetic signals scattering from radar targets have been well studied for the last few decades. In the late 1960s, Kennaugh [20] first extended the concept of impulse response from circuit theory to transient electromagnetic scattering. Later in the 1970s, Baum [16] extended the concept and formulated the Singularity Expansion Method (SEM), which mathematically describes the transient scattering phenomena. In general, the target scattered transient can generally be divided into two intervals: the early and late time. The early time response is difficult to model due to the fact that in the early time the excitation electromagnetic pulse has not fully excited the target. As a result, the early time response is dependent on the incident aspect angle and scattering phenomena in the early time is considered to be local. In general the early time response is dominated by the specular returns from the target. Studies have found that the early time response can either be modelled using the frequency dependent coupling coefficients associated with the damped exponential model [21] or a series of entire functions [22].

The SEM describes the late time of the transient target signature as a sum of damped exponential with Complex Natural Resonances (CNRs). Mathematically it can be written as [18]

$$r(t) = \sum_{n=1}^{N} A_n e^{s_n t} + A_n^* e^{s_n^* t}, \; t > T_l \tag{1}$$

where A_n is the aspect dependent amplitude of the n^{th} mode and T_l is the onset of the late time period. With the known target, the late time can be approximated by

$$T_l = T_b + T_p + 2T_{tr} \tag{2}$$

where T_b is the estimated edge when the waves strikes the leading edge of the target, T_p is the effective pulse duration and T_{tr} is the maximal transit time of the target [19]. In equation (1), it is assumed that only N modes are excited by the incident field. The * sign denotes the complex conjugate. The CNRs are given by $s_n = \sigma_n \pm j\omega_n$, where σ_n and ω_n are the damping coefficients and resonant frequencies respectively. These late time resonances occur when the pulse has been propagated past the whole target, and as such is fundamentally a global phenomenon (rather than a collection of local interactions) Theoretically these complex resonances correspond purely to the physical properties of the target's geometry, dielectric properties and loss mechanisms. They are also theoretically aspect independent [18] and independent of the incident wave polarization state [23]. Target recognition schemes that make use of such target dependent resonances as a feature set have been widely addressed and may be found in the literature, for example [18-19].

Equation (1) describes the scattering behaviour in the late time. A more precise description was given by Heyman [24] in that each resonant component has its own 'turn-on' time [24]. The late time is essentially the time when all of these resonances have been established. However, each resonance may commence at a different time. In addition, Heyman [23] also mentions that the resonance phenomena can be considered as a consequence of the multiple interactions of the dominant scattering mechanisms such as edge and corner diffraction and creeping wave diffractions, and thus a hybrid wavefront SEM model describing the late time response has been proposed. The timing for each of these scattering phenomena is also target and aspect dependent, and could be complicated when some of these occur concurrently.

Extensions from equation (1) together with the introduction of a "turn-on" time concept by Heyman, recent efforts by Jang [22] have resulted in a series of Gaussian functions to model the early time together with the damped exponential model for the late time. The search for optimum parameters ("turn-on" times of each CNR, residues, amplitude and time shift of the Gaussian pulse) can be achieved using quasi-Newton approach [22]. As demonstrated, such UWB electromagnetic transients are therefore highly non-stationary in both early and late time and thus TF analysis is more applicable compared to standard Fourier analysis.

III. TIME - FREQUENCY ANALYSIS

The motivation of TF analysis originates from the nature of non-stationary signals, where the frequency components of the signals are time variant. In this work, we focus on applying TFDs to studying the temporal occurrence of frequency, which corresponds to certain scattering phenomena of the radar target. Our main objective is to make use of TFDs as a tool to produce a meaningful image which can clearly reveal all scattering phenomena. As a result, we will focus on some well-known TFDs that are suitable for our applications.

One of the most well known TFDs is the STFT. Compared to standard Fourier analysis which takes the entire duration of the signal in time and then takes the transform, the signal is first windowed with a time-limited window and then transformed to the frequency domain via a Fourier Transform. The STFT is essentially a windowed version of the Fourier transform, which considers the frequency spectrum within a short period of time. One of the drawbacks of the STFT is that time and frequency resolution cannot be simultaneously achieved, due to the uncertainty principle [1-4]. This can be handled by using the Continuous Wavelet Transform (CWT) which results in multi-resolution in the TF domain. Previous work by H. Ling et al. [13-15] on TF analysis of transient electromagnetic scattering has demonstrated the advantages on using CWT over STFT. Summaries using TF analysis for electromagnetic scattering using CWT can be found in [13].

Another TFD that is capable of handling the limited TF resolution is known as the Wigner-Ville Distribution (WVD) [1-4]. Mathematically the WVD of the signal $x(t)$ can be written as

$$W_x(t,v)=\int_{-\infty}^{+\infty} x_a(t+\tau/2)x_a^*(t-\tau/2)e^{-j2\pi v\tau}d\tau \qquad (3)$$

where x_a is the analytic signal of $x(t)$. One of the strongest features of the WVD is that it is able to produce the best time and frequency resolution simultaneously amongst all members of the Cohen class [1-2] for signals with a single component. However, for signals with multi-components, the WVD suffers from so-called cross-term interference [5]. These cross terms appear only when the signal is made up of more than one component. Consider the case of two components. Due to the quadratic superposition principle, the WVD of the signal $x_1(t)+x_2(t)$ is equal to the sum of the WVD of $x_1(t)$ and $x_2(t)$ individually, together with the WVD of the product of $x_1(t)$ and $x_2(t)$. Mathematically it can be written as

$$W_{x_1+x_2}(t,v)=W_{x_1}(t,v)+W_{x_2}(t,v)+2\,\mathrm{Re}\left[W_{x_1x_2}(t,v)\right] \qquad (4)$$

where

$$W_{x_1x_2}(t,v)=\int_{-\infty}^{+\infty} x_1(t+\tau/2)x_2^*(t-\tau/2)e^{-j2\pi v\tau}d\tau \qquad (5)$$

is the cross WVD of $x_1(t)$ and $x_2(t)$, and is also known as the cross term [3, 5]. The $W_{x_1}(t,v)$ and $W_{x_2}(t,v)$ are the WVD of $x_1(t)$ and $x_2(t)$ respectively and are known as auto terms. The cross-term interference is troublesome as it may overlap with the auto-terms thus making it difficult to visually interpret the WVD image.

For most engineering and signal analysis applications these cross terms do not provide any physical meaning. As a result work has been done to suppress them. These include using the smooth versions of WVD [5]. If we consider windowing the WVD using a rectangular window $h(t)$ in the time domain, or equivalently writing the resultant distribution as

$$PW_x(t,v)=\int_{-\infty}^{+\infty} h(\tau)x_a(t+\tau/2)x_a^*(t-\tau/2)e^{-j2\pi v\tau}d\tau \qquad (6)$$

which is known as the Pseudo Wigner-Ville Distribution (PWVD). If we add another degree of freedom by considering a separable smoothing function $g(t)$, the Smooth Pseudo Wigner-Ville Distribution (SPWVD) can be written as

$$SPW_x(t,v)=\int_{-\infty}^{+\infty} h(\tau)\left[\int_{-\infty}^{+\infty} g(s-t)\,x_a(s+\tau/2)x_a^*(s-\tau/2)ds\right]e^{-j2\pi v\tau}d\tau\ . \qquad (7)$$

The SPWVD was first proposed by Flandrin [5] in 1984. It has been demonstrated that the SPWVD is capable of suppressing the cross-term interference. However, throughout the smoothing window operation, time and frequency localization are reduced.

Another common approach to suppressing cross-term interference is to use a specially designed kernel [6-9]. Such a kernel is specially designed such that it is capable of suppressing the cross terms, at the same time maintaining the desirable properties of the TFDs. The exponential kernel and the cone-shaped kernel are the most well known kernels for cross-term suppression, and the corresponding distributions are well known as the Choi-William Distribution (CWD) [6] and Zhao-Atlas-Marks Distribution (ZAMD) [7-8]. Details on CWD and ZAMD are not covered here and they can be found in corresponding references.

In addition to smoothing the WVD and designing special kernels, there are various approaches to reducing the cross-term interference at the same time maintaining good TF resolution. These include using Time-Frequency Distribution Series on WVD [25], improving TF localization using reassignment method [26], and improving TF resolution using time-scaled/affine TFDs [27]. Due to the limited scope of this paper, these methods will not be covered. A general review for TFDs can be found in [1-4] and details on particular approach on improving TFDs can be found in the corresponding references.

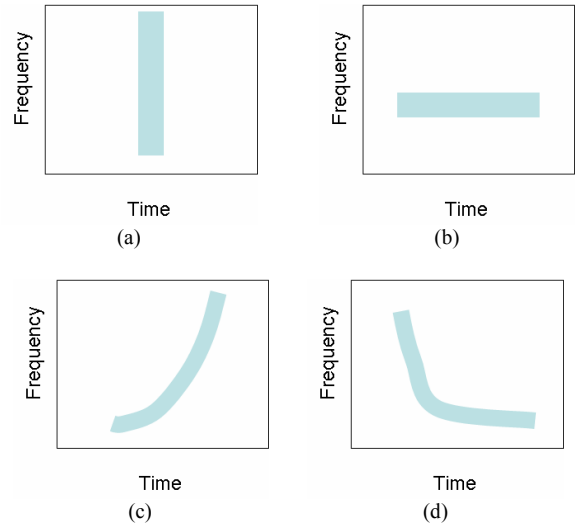

Fig. 1. Electromagnetic Scattering Mechanism manifested in the Time-Frequency domain, (a) wavefront; (b) resonance; (c) material dispersion and (d) structural dispersion [13]

TF analysis on electromagnetic scattering was first addressed by H. Ling et al. in a number of works [13-15]. According to [13], different scattering mechanism will appear differently in the TF domain. The four main scattering phenomena are shown in Figure 1 (a) to (d). A vertical line in the TF domain indicates that the scattering event occurs for a particular time instant but over all frequencies, which corresponds to a wavefront phenomena or scattering centre (Figure 1(a)). A horizontal line in the TF domain indicates that the scattering phenomenon dominates in a particular frequency over the time frame, which corresponds to resonance (Figure 1(b)). Dispersive phenomena,

however, will be appeared as slopes in the TF domain. A positive slope in the TF domain corresponds to surface wave mechanism due to material coating (Figure 1(c)), and a negative slope corresponds to structure dispersion (Figure 1(d)). In the numerical examples we will focus on the scattering wavefront and resonance phenomena in the TF domain.

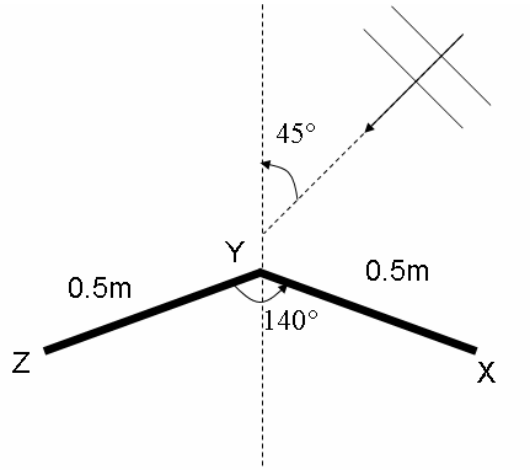

Fig. 2. Bent wire target under plane wave excitation in free space

IV. NUMERICAL EXAMPLES

A numerical example for the bent wire target shown in Figure 2 will be considered. It is made up of two sections of PEC wire segments each of length 0.5m and included angle of $140°$. The ends of the wire segment on the right and left hand side are denoted as Point X and Z respectively, and the junction of the two wire segments is denoted as Point Y. Plane wave incidence at $45°$ with the electric field polarized in plane of the target is considered. The study of scattering for a straight thin wire in the time domain has been treated in the electromagnetic context by Shamansky [28] using the Method of Moments (MoM) and GTD. Instead of a straight wire target, here the scattering path on the bent wire target is considered as shown in Figure 3. Figure 3 (a) shows the scattering events A, B and C, which correspond to the specular reflection from points X, Y, and Z respectively. Event D corresponds to case which the electromagnetic pulse strikes at point X, surface wave propagates on the surface of the wire segment XY and diffracts off at point Y. Similarly, event E corresponds to the case which the pulse strikes at point Z, surface wave propagates on the surface of the wire segment YZ and diffracts off at point Y. Event F corresponds to the case which the pulse strikes on point Z, surface wave travels through the entire target and diffracts off at point X. Event G corresponds to the case which the pulse strikes on point X, and the surface wave travels one round trip through the entire target, and event H corresponds to the case which the electromagnetic pulse strike on point Z, surface wave propagates through the entire target and diffracts off at point Y. Lastly, event I corresponds to the case which the electromagnetic pulse has propagated two round trips.

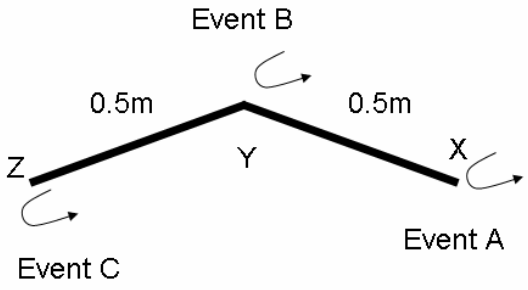

(a) Events A to C

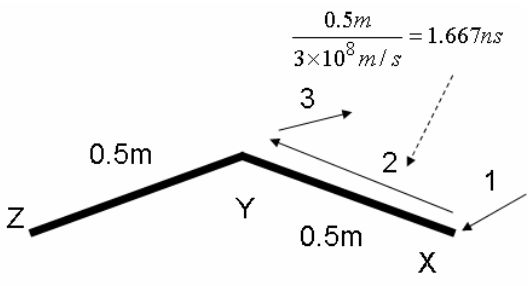

(b) Event D

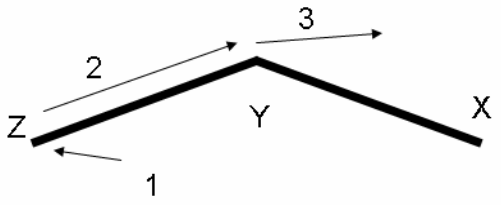

(c) Event E

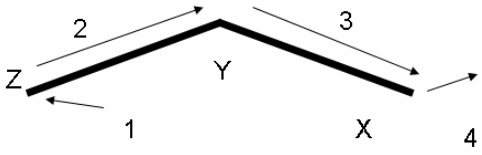

(d) Event F

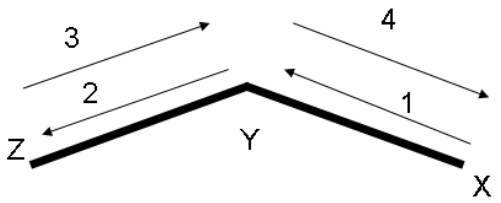

(e) Event G

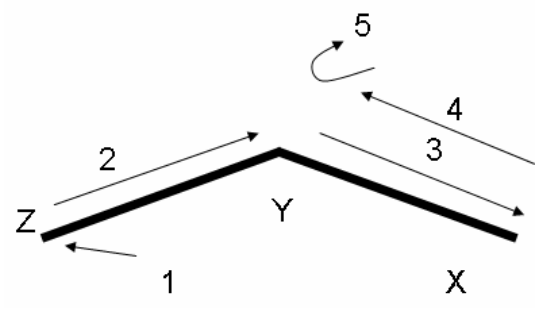

(f) Event H

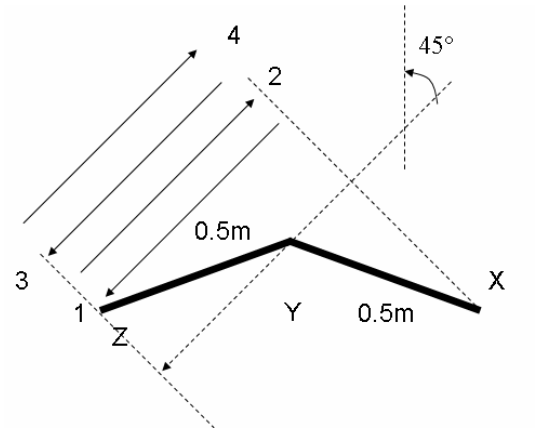

(g) Event I

Fig. 3. Scattering Path of the Bent Wire target

With the Gaussian pulse striking the target at 10ns together with an incident angle of 45° , the pulse first hits the right side of the target at point X, followed by the centre at point Y and lastly the end of the wire segment on the left hand side at point Z. The time required for the electromagnetic pulse travelling from Point X to Point Y and Point X to Point Z are shown in Figure 4. The occurrence of each scattering events shown in Figure 3 are calculated and listed in Table 1.

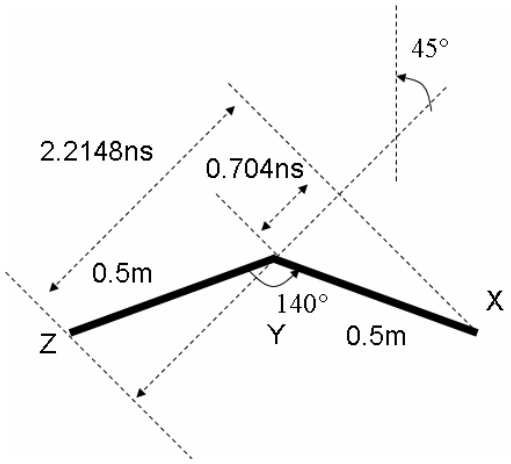

Fig. 4. Time required for the electromagnetic pulse travelled from Point X to Y and Z

TABLE I
TIMING OF THE SCATTERING EVENTS APPEARED ON THE TARGET RESPONSE

Event	Time when the wave appears on the target response
A	$t_0 = 10ns$
B	$t_0 + (2 \times 0.704ns) = 11.408ns$
C	$t_0 + (2 \times 2.2148ns) = 14.4296ns$
D	$t_0 + 1.667ns + 0.704ns = 12.371ns$
E	$t_0 + 2.2148ns + 1.667ns + 0.704ns = 14.585ns$
F	$t_0 + 2.2148ns + (2 \times 1.667ns) = 15.549ns$
G	$t_0 + (4 \times 1.667ns) = 16.668ns$
H	$t_0 + 2.2148ns + (3 \times 1.667ns) + 0.704 = 17.920ns$
I	$t_0 + (4 \times 2.2148ns) = 18.860ns$

To study the transient scattering behaviour, it is required to obtain the transient target response either by measurement or numerical modelling. In this work numerical modelling is considered. The target response is first computed in the frequency domain using a commercial MoM solver FEKO [29] from 976MHz to 9GHz with 2048 equal spaced samples. The frequency response is then windowed by a Gaussian shaped window which corresponds to the Gaussian Pulse in time domain. The Gaussian pulse is used as the time domain illuminating wave shape in all case and acts an approximation to the impulse response [30]. The target response in time domain is then achieved by applying an inverse Fourier Transform to the frequency response.

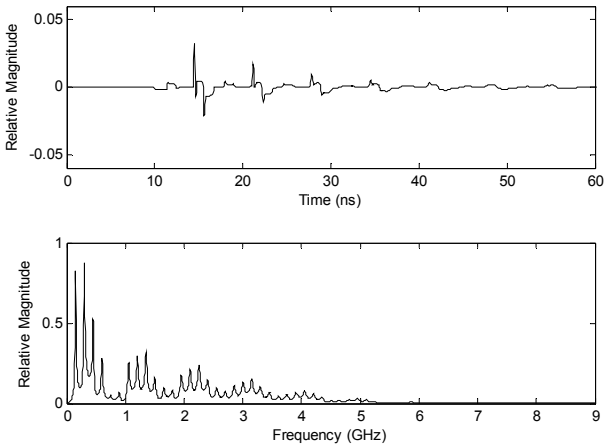

Fig. 5. Target responses in time and frequency domain

The target responses in time and frequency domain are shown in Figure 5. In time domain, the electromagnetic pulse strikes on the target at 10ns. As the target is a PEC, electric current is induced on the surface of the target according to the boundary conditions of the Maxwell's equation [16]. The electric current acts as a source and re-radiates the electromagnetic field. As a result, the first specular return is observed at 10ns and a series of scattering events occur thereafter. In the frequency domain, a number of high-Q resonant peaks are observed. The first few dominant resonant

peaks with large magnitudes are located below 1GHz in the frequency response.

To clearly identify the occurrence of the scattering events shown in Figure 3 and listed in Table 1 in the time domain response, a zoom-in version of the target response from 9.5ns to 20ns is shown in Figure 6 with the scattering events marked. However, this does not provide any further information or insight about the scattering behaviour (either time or frequency) of these events.

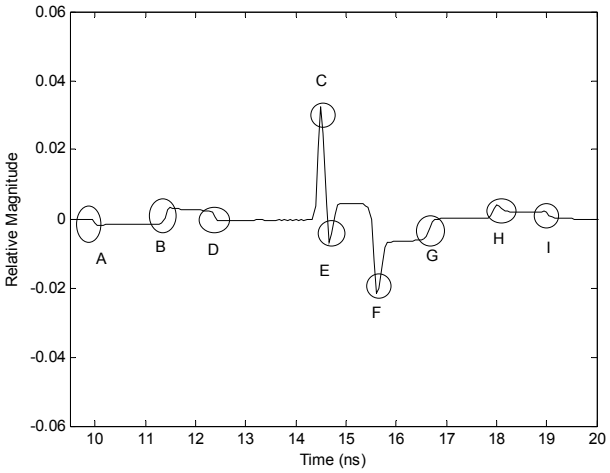

Fig. 6. Target responses in time domain from 9.5ns to 20ns

To gain further insights into the transient scattering, TF analysis is considered. The TFDs of the target response from 9.44ns to 20ns is considered and shown in Figure 7 to 12. According to equation (2), with $T_b = 10ns$, $T_p = 0.22ns$ and $T_{tr} = 2.2148ns$, commencement of the late time period is calculated to be 14.65ns. As a result, the time frame of 9.44ns to 20ns covers both the early time period as well as the commencement of the late time period. As expected, events A to I are clearly observed as vertical lines in the TF plots. This indicates that these events correspond to scattering wavefronts. It is worth noting that some of them interact with each other resulting in partial resonances in the early time period and global resonances in the late time period. Such observations are in accordance with the hybrid wavefront SEM model [24], in that the resonances can also be considered as the consequence of multiple interactions between individual wavefronts.

Comparing between various TFDs, poor TF resolution is observed in the SP shown in Figure 7. The WVD does enhance the resolution, however, cross-term interference appear as vertical lines occurs between 12ns to 14ns. These lines only appear in the WVD but not in other TFDs, which confirm that they are the cross-term interferences. The cross terms can be suppressed by smoothing the WVD, resulting the PWVD and SPWVD shown in Figure 9 and 10. The cross terms can also be suppressed using special designed kernel such as the exponential and cone shaped kernel and their corresponding distributions are also shown in Figure 11 and 12 respectively. It is worth noting that the SPWVD, CWD and ZAMD shown in Figure 10, 11 and 12 respectively all demonstrate good cross-term suppression. This can be verified by comparing them with the SP shown in Figure 7 as it is well known that SP does not suffer from any cross-term interference.

In addition to cross-term suppression, the SPWVD, CWD and ZAMD results indicate better TF resolution than the SP. However, the CWD suffers from interference when there are synchronized components in the TF domain. As shown in Figure 11, there exists more than one frequency component when scattering events A to I occurs, and thus eight vertical lines are clearly observed from DC up to 9GHz (events C and E appeared as one line). These vertical lines appear up to 6GHz only for other TFDs. As a result, we can conclude that the vertical lines from 6GHz and above shown in Figure 11 are the interference components.

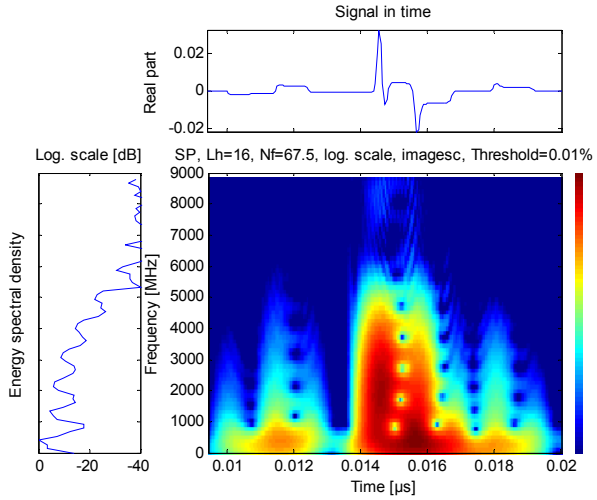

Fig. 7. SP of the time target response from 9.44ns to 20ns

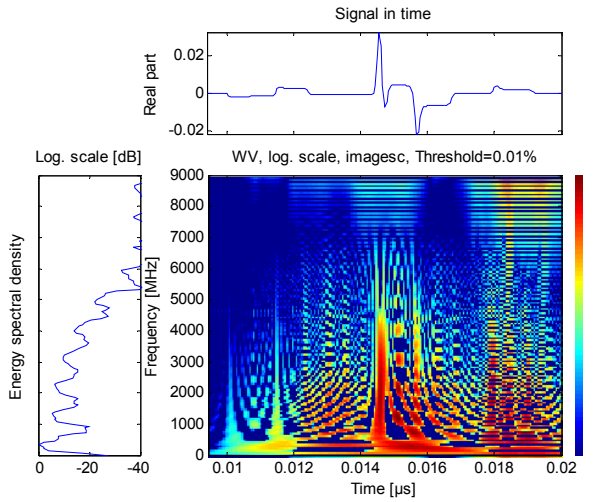

Fig. 8. WVD of the time target response from 9.44ns to 20ns

Lastly, it is also worth noting that the vertical line corresponds to scattering events C and E shown at 14.5ns. As shown in the SP, WVD, PWVD and SPWVD, higher energy level (red) is observed up to about 4.5GHz and a relative lower energy level (yellow) is shown from 4.5GHz up to 6GHz However, in the ZAMD shown in Figure 12, only the high

energy level up to 4GHz is shown. This seems to indicate that the cone-shaped kernel may also suppress some of the low energy level components in the TF domain.

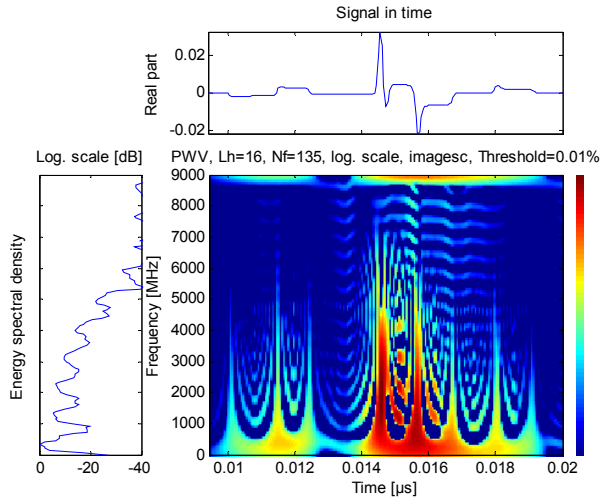

Fig. 9. PWVD of the time target response from 9.44ns to 20ns

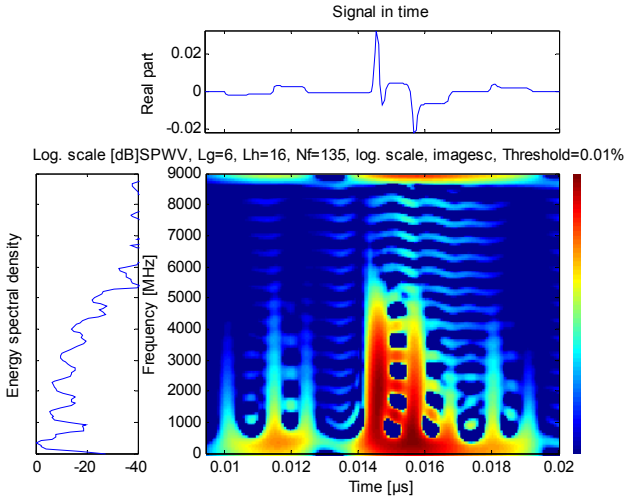

Fig. 10. SPWVD of the time target response from 9.44ns to 20ns

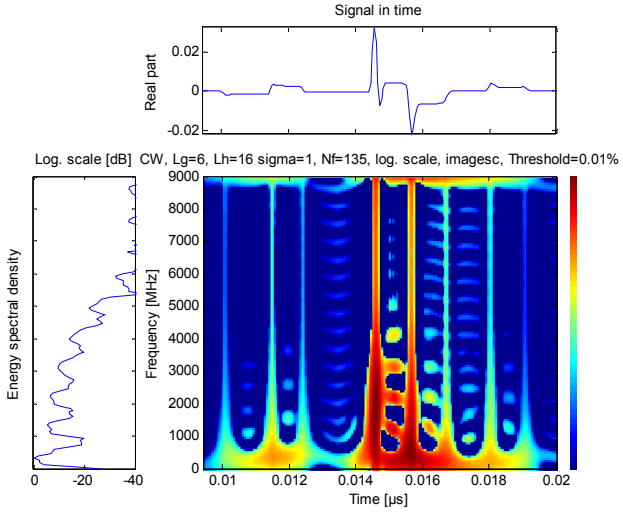

Fig. 11. CWD of the time target response from 9.44ns to 20ns

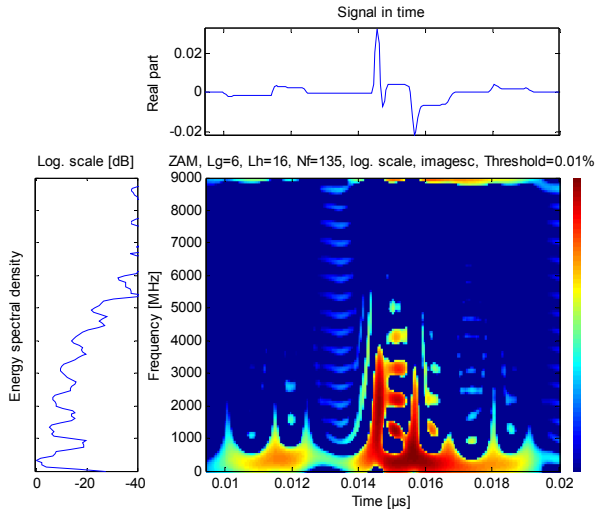

Fig. 12. ZAMD of the time target response from 9.44ns to 20ns

After considering the issues on TF resolution as well as artefacts (interference) introduced by TFDs, a small conclusion can be reached that the SPWVD and the ZAMD are suitable candidates for studying the transient electromagnetic scattering phenomena in the TF domain in this example. They are both immune to interference and at the same time maintaining reasonable TF resolution.

V. CONCLUSION

In this paper, Joint TF analysis of UWB radar signals has been carried out. Numerical examples for a bent wire target have demonstrated the feasibility of using TFDs to study the transient electromagnetic scattering phenomena from a PEC radar target. The electromagnetic scattering mechanisms are first identified in the time domain and further investigated in the TF domain. In this example, the focus has been on specular reflections in early time period and various wavefront interactions in the late time period. It has also been clearly observed that some of the wavefront phenomena interact with each other resulting in partial resonances. Such observations are in line with the conclusion given by Heyman and Felsen [24] using a hybrid wavefront SEM model. Studies on transient electromagnetic scattering using TFDs presented here further verifies that the hybrid wavefront SEM model provides further physical insight than the original SEM model.

Comparisons of various TFDs for the same transient signal have also been carried out. Results demonstrate that the WVD is not suitable for this particular application as it suffers severely from cross-term interference. This is due to the fact that in this example the target itself is a high-Q scatterer and its target response is made up of a number of resonant and wavefront components. Various TFDs capable of suppressing cross-term interference have been considered. It is found that the SPWVD and ZAMD are preferred for this example which also maintains a reasonable TF resolution to reveal various scattering mechanisms in the TF domain.

Lastly, the example presented in this paper is a bent wire target, which is a two dimensional electromagnetic scattering

problem. For the electromagnetic researcher, future work will focus on studying the scattering phenomena using TFDs on more complicated three dimension PEC targets and dielectric targets, which may potentially lead to deeper insight of the scattering physics.

ACKNOWLEDGMENT

The authors acknowledge the Australian Research Council (ARC) that partially supports this work under grant number DP0557169.

REFERENCES

[1] L. Cohen, "Time-frequency distributions – A review," *Proc. IEEE*, Vol. 77, No. 7, pp. 941-979, 1989.

[2] L. Cohen, *Time-Frequency Analysis.* Englewood Cliffs, NJ: Prentice Hall, 1995.

[3] B. Boashash, Ed., *Time-Frequency Signal Analysis: Methods and Applications, Melbourne*; Longman; Cheshire, 1992.

[4] B. Boashash, Ed., *Time-Frequency Signal Analysis and Processing – A Comprehensive Reference,* Amsterdam; Boston: Elsevier, 2003.

[5] P. Flandrin, "Some features of time-frequency representations of multicomponent signals", in the *Proc. IEEE Int. Conf. Acoustic, Speech, Signal Processing, ICASSP-84*, pp. 41B.4.1 – 41B.4.4, San Diego, CA, 1984.

[6] H. Choi, W. J. Williams, "Improved Time-Frequency Representation of Multicomponent Signals Using Exponential Kernel", *IEEE Trans. Acoustics, Speech and Signal Processing,* Vol. 37, No. 6, pp. 862-871, June 1989.

[7] Y. Zhao, L. E. Atlas, R. J. Marks, "The Use of Cone-Shaped Kernels for Generalized Time-Frequency Representations of Nonstationary Signals", *IEEE Trans. Acoustics, Speech and Signal Processing,* Vol. 38, No. 7, pp. 1084-1091, July 1990.

[8] S. Oh, R. J. Marks, "Some Properties of the Generalized Time Frequency Representation with Cone-Shaped Kernel", *IEEE Trans. Signal Processing,* Vol. 40, No. 7, pp. 1735-1745, July 1992.

[9] J. Jeong, W. J. Williams, "Kernel Design for Reduced Interference Distribution", *IEEE Trans. Signal Processing,* Vol. 40, No. 2, pp. 402-412, February 1992.

[10] G. C. Gaunard, H. S. Strifors, "Signal Analysis by means of Time-Frequency (Wigner-Type) Distributions – Applications to Sonar and Radar Echoes", *Proc. IEEE*, Vol. 84, No. 9, pp. 1231-1248, September 1996.

[11] G. Turhan-Sayan, "Natural Based Feature Extraction with Reduced Aspect Sensitivity for Electromagnetic Target Classification", *Pattern Recognition* 36, pp. 1449-1466, 2003.

[12] G. Turhan-Sayan, "Real Time Electromagnetic Target Classification Using a Novel Feature Extraction technique with PCA-Based Fusion", *IEEE Trans. Antennas & Propagation*, Vol. 53, No. 2, pp. 766-776, February 2005.

[13] V. C. Chen, H. Ling, *Time-Frequency Transforms for Radar Imaging and Signal Analysis*, Artech House, Boston, MA, 2002.

[14] H. Kim, H. Ling, "Wavelet Analysis of Electromagnetic Backscatter Data", *Electronics Letters*, Vol. 28, No. 3, pp. 279-281, January 1992.

[15] H. Ling, H. Kim, "Wavelet Analysis of Backscattering Data from an Open-Ended Waveguide Cavity", *IEEE Microwave and Guided Wave Letters*, Vol. 2, No. 4, April 1992.

[16] C. A. Balanis, *Advanced Engineering Electromagnetics*, John Wiley & Sons, 1989.

[17] C. E. Baum, "The Singularity Expansion Method" *in Transient Electromagnetic Fields*, L.B. Felsen Ed., New York Springer-Verlag, pp. 129-179, 1976.

[18] C. E. Baum, E. J. Rothwell, K. M. Chen, D. P. Nyquist, "The Singularity Expansion Method and Its Application to Target Identification", *Proc. IEEE*, Vol. 79, No. 10, pp. 1481-1491, October 1991.

[19] P. Ilavarasan, J.E. Ross E.J. Rothwell, K.M. Chen & D. P. Nyquist, "Performance of an Automated Radar Target Pulse Discrimination Scheme Using E pulses and S Pulses", *IEEE Trans. Antennas & Propag,* Vol. 41, No.5, pp 582-588, May, 1993.

[20] E. M. Kennaugh, D. L. Moffatt, "Transient and Impulse Response Approximations" *Proc. IEEE*, pp. 893-901, August 1965.

[21] M. A. Richards," SEM Representations of the Early and Late Time Fields Scattered from Wire Targets", *IEEE Trans. Antennas & Propag.*, Vol. 42, No.4, pp. 564-566, April, 1994.

[22] S. Jang, W. Choi, T. K. Sarkar, M. Salazar-Palma, K. Kim, C. E. Baum, "Exploiting Early Time Response Using The Fractional Fourier Transform for Analyzing Transient Returns", *IEEE Trans. Antennas & Propag.*, Vol 52, No. 11, pp. 3109-3119, November 2004.

[23] N. Shuley, D. Longstaff, "Role of Polarisation in Automatic Target Recognition using Resonance Descriptions", *Electronics Letters*, Vol. 40, No. 4, pp. 268-270, February 2004.

[24] E. Heyman, L. B. Felsen, "A Wavefront Interpretation of the Singularity Expansion Method", *IEEE Trans. Antennas & Propag,* Vol. 33, No. 7, pp. 706-718, July 1985.

[25] S. Qian, D. Chen, "Decomposition of the Wigner-Ville Distribution and Time-Frequency Distribution Series", *IEEE Trans. Signal Processing,* Vol. 42, No. 10, pp. 2836-2842, October 1994.

[26] F. Auger, P. Flandrin, "Improving the Readability of Time-Frequency and Time-Scale Representations by the Reassignment Method", *IEEE Trans. Signal Processing,* Vol. 43, No. 5, pp. 1068-1088, May 1995.

[27] O. Rioul, P. Flandrin, "Time-Scale Energy Distributions: A General Class Extending Wavelet Transform", *IEEE Trans. Signal Processing,* Vol. 40, No. 7, pp. 1746-1757, July 1992.

[28] H. T. Shamansky, A. K. Dominek, L. Peters, "Electromagnetic Scattering by a Straight Thin Wire", *IEEE Trans. on Antennas & Propag.,* Vol. 37, No. 8, pp. 1019-1025, August, 1989.

[29] FEKO EM Software & Systems S.A., (Pty) Ltd, 32 Techno Lane, Technopark, Stellenbosch, 7600, South Africa.

[30] S. M. Rao, *Time Domain Electromagnetics*, Academic Press, 1999.